Supplemental Materials for "Tunable abundant valley Hall effect and chiral spin-valley locking in Janus monolayer $VCGeN_4$"

Kang Jia[1,2], *Xiao-Jing Dong*[2], *Sheng-Shi Li*[1], *Wei-Xiao Ji*[1], *and Chang-Wen Zhang*[1,2*]

1. School of Physics and Technology, Institute of Spintronics, University of Jinan, Jinan, Shandong, 250022, PRC
2. School of Physics and Physical Engineering, Qufu Normal University, Qufu, Shandong, 273100, PRC

Table S1 The energies of different phases of $VCGeN_4$.

phase	energy (eV)
α	-50.774
β	-50.694
γ	-50.669
δ	-50.769

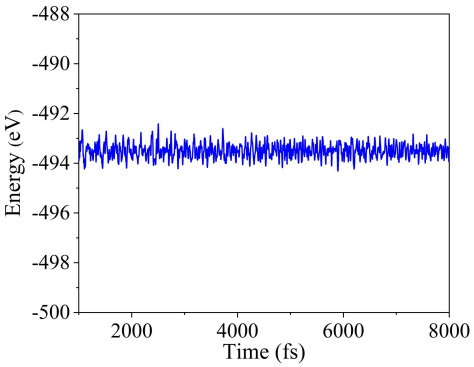

Fig. S1 The AIMD simulation of $VCGeN_4$ at 300 K.

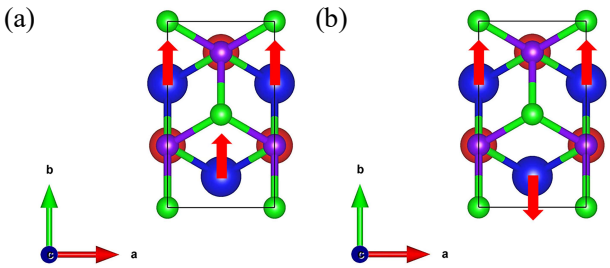

Fig. S2 The considered magnetic configurations: panel (a) is for the FM configuration, and panel (b) is for the AFM configuration.s

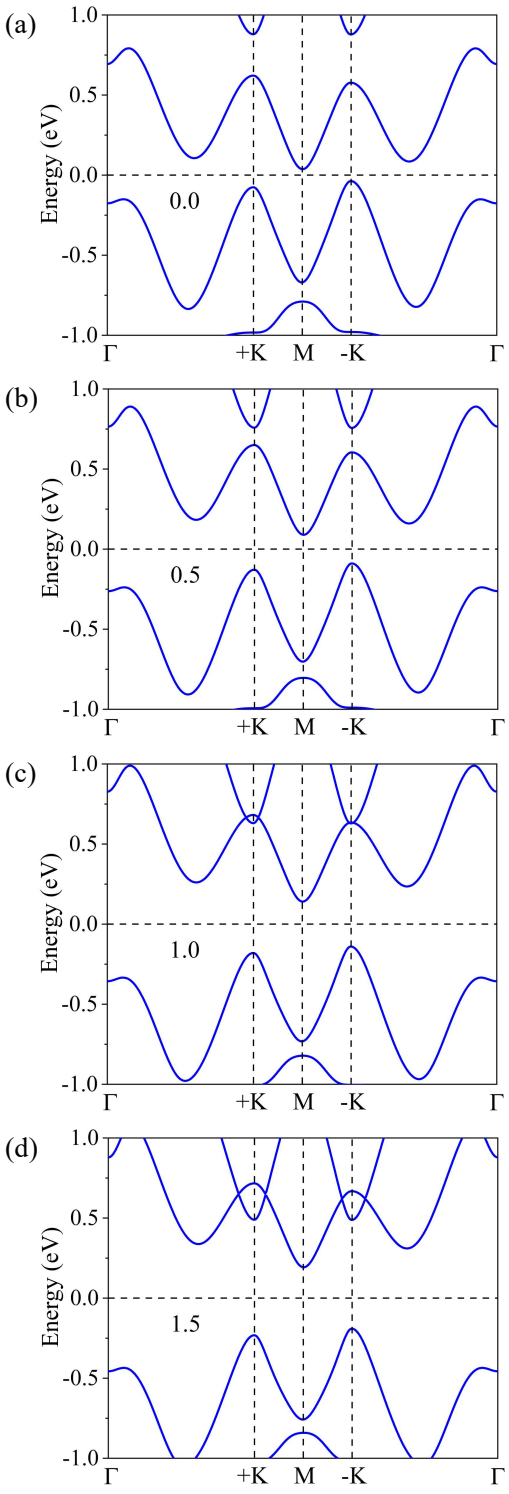

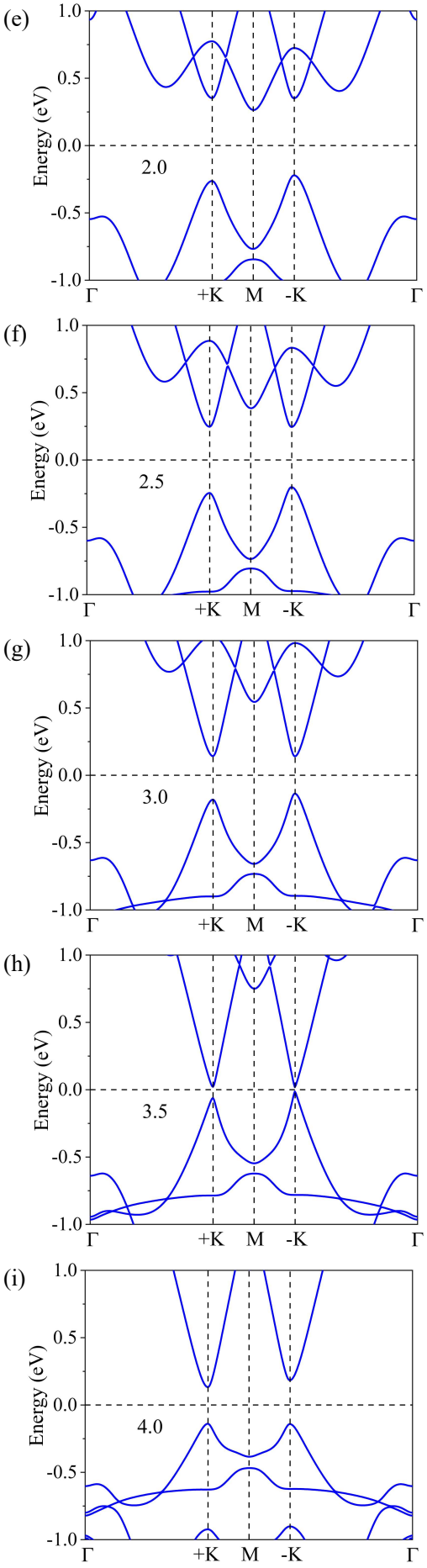

Fig. S3 The band structures of the $VCGeN_4$ gained from PBE+U method (U values vary from 0.0 to 4.0 eV) with OOP magnetization.

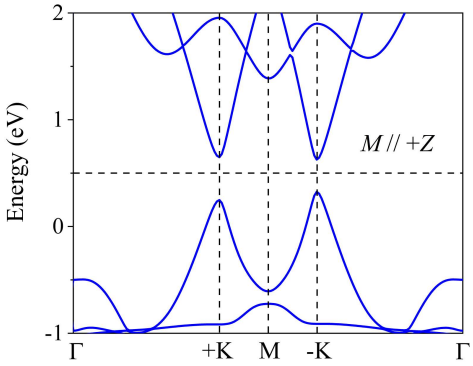

Fig. S4 The band structure of the $VCGeN_4$ by the HSE06 functional with OOP magnetization.

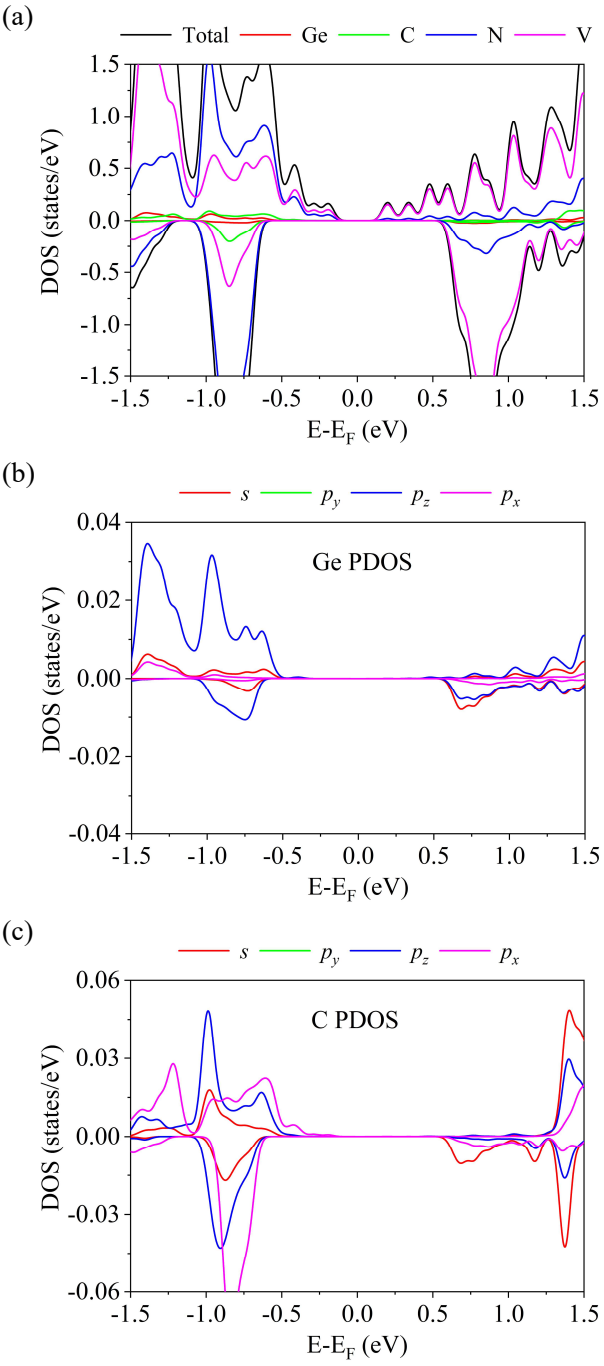

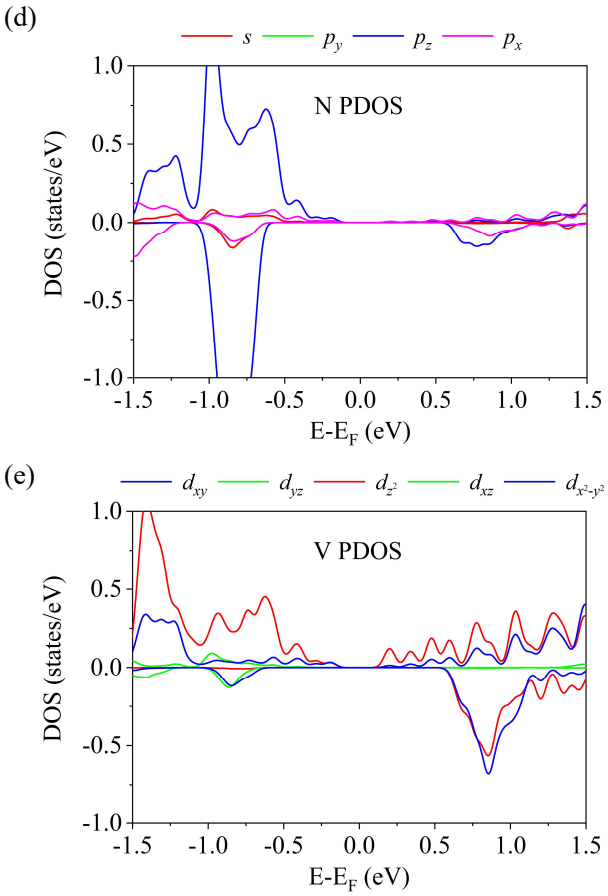

Fig. S5 (a) The total density of states (DOS) of the $VCGeN_4$. (b) The partial density of states (PDOS) of Ge atoms. (c) The PDOS of C atoms. (d) The PDOS of N atoms. (e) The PDOS of V atoms.

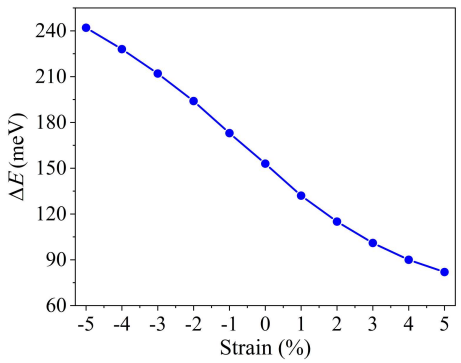

Fig. S6 The energy differences (ΔE = E_{AFM} - E_{FM}) between FM and AFM configurations of $VCGeN_4$ as a function of strain.

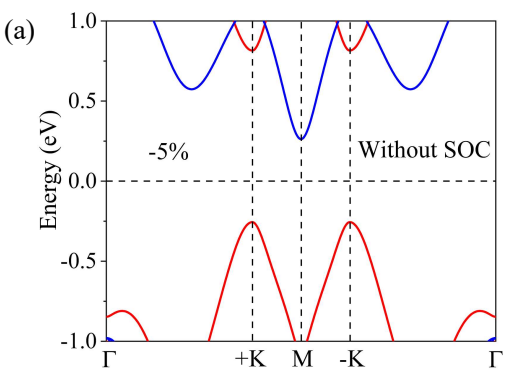

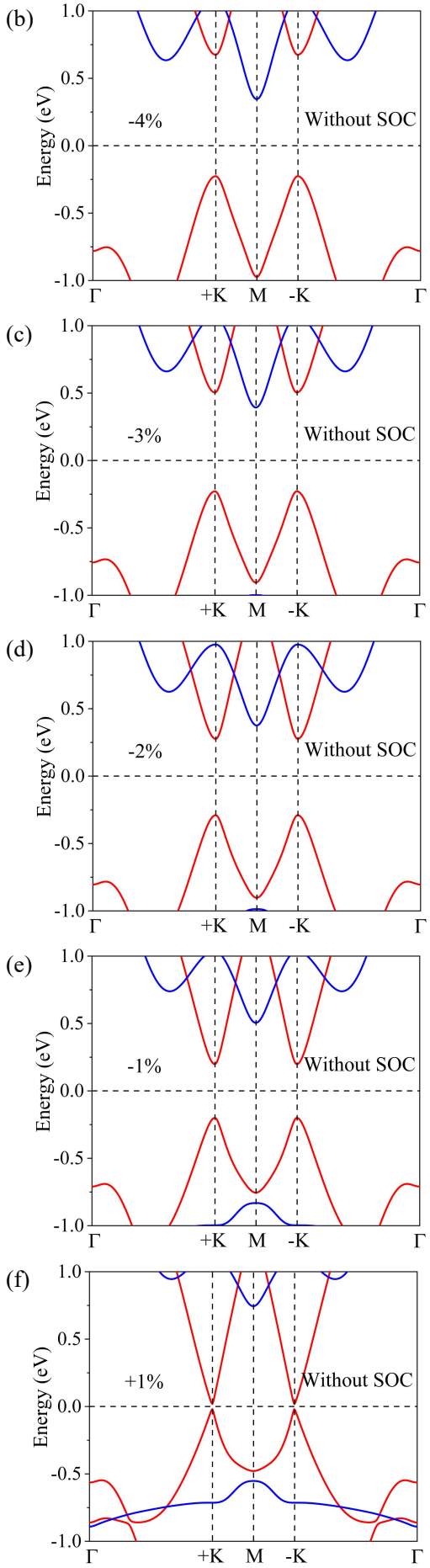

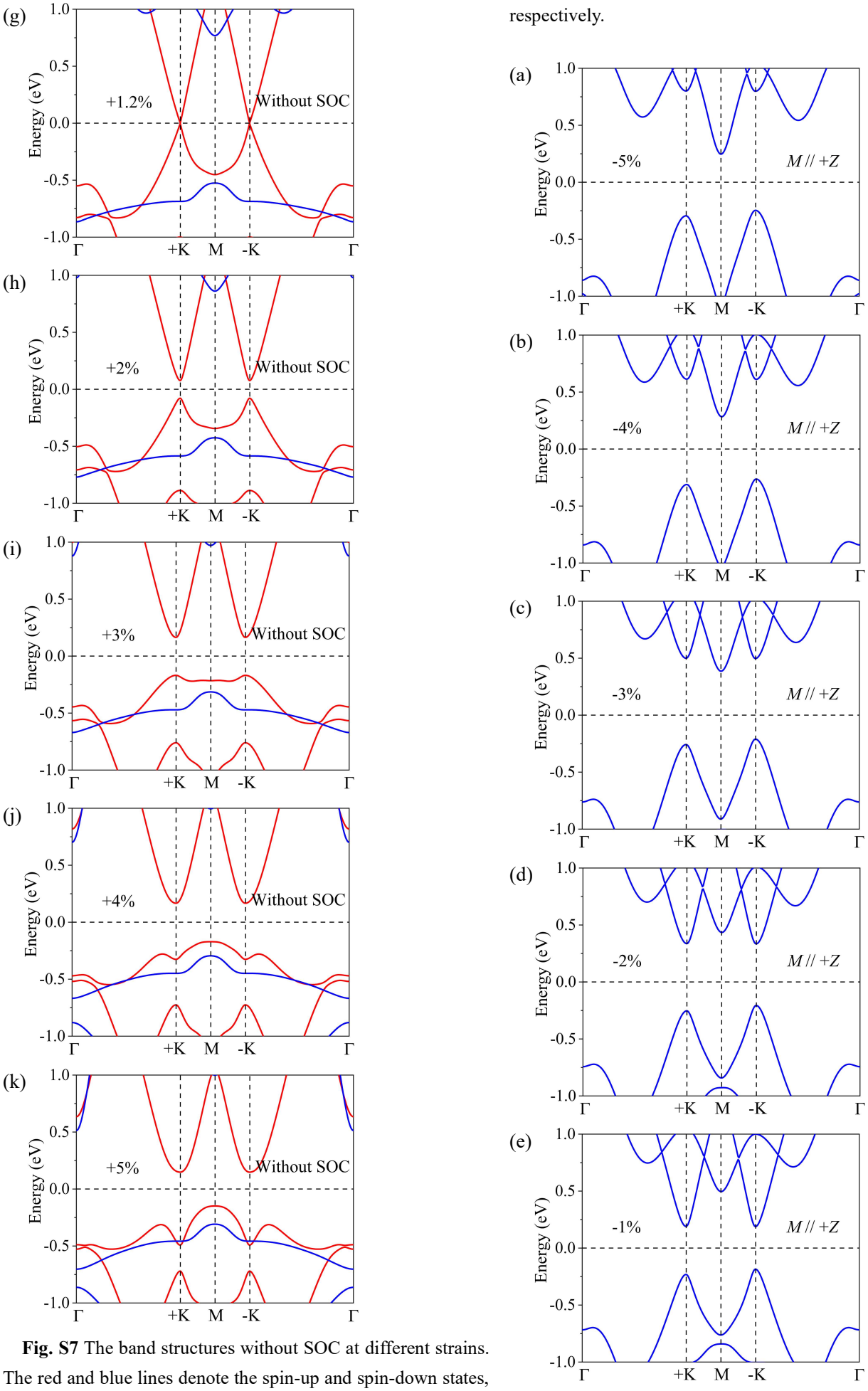

Fig. S7 The band structures without SOC at different strains. The red and blue lines denote the spin-up and spin-down states, respectively.

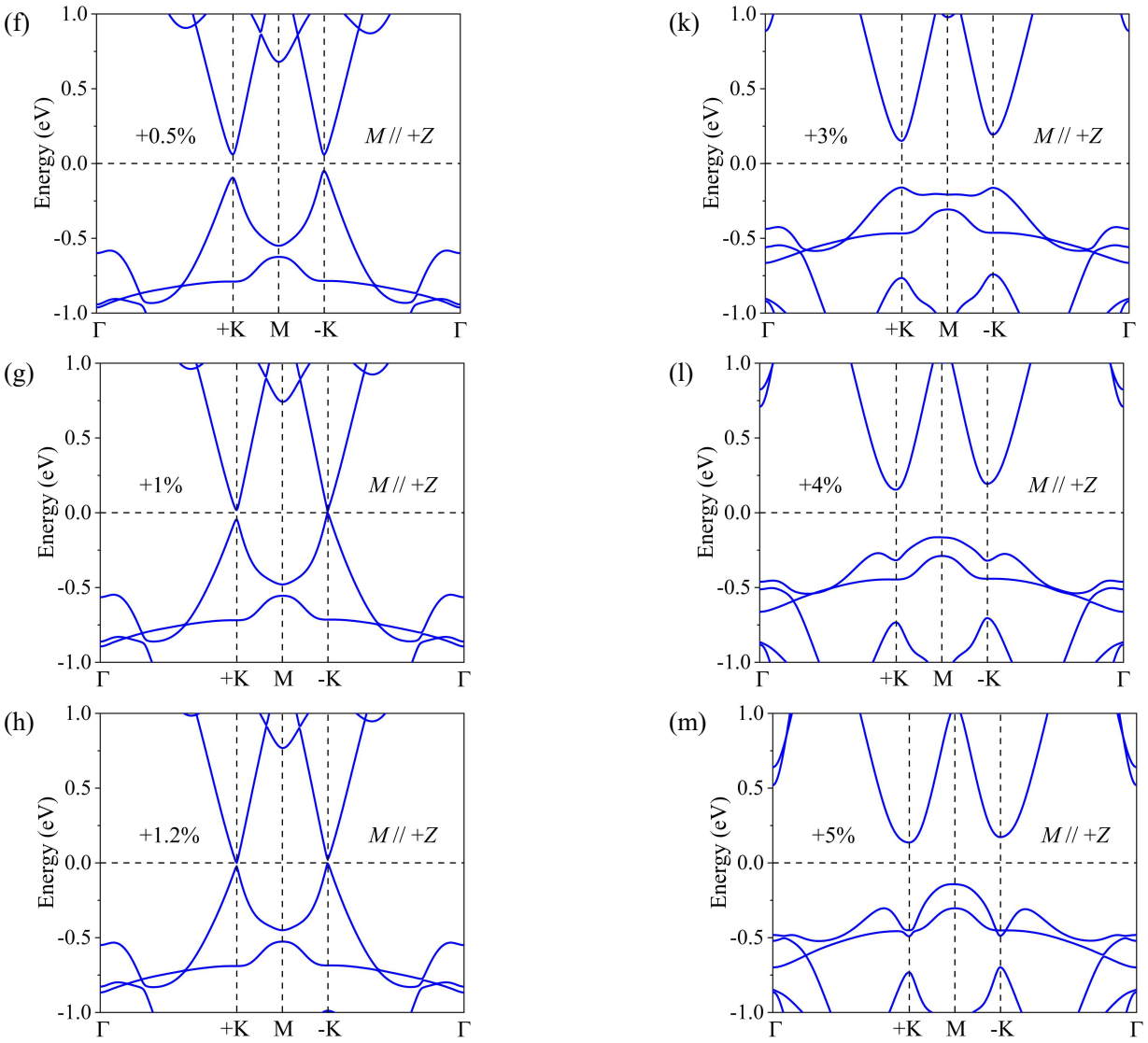

Fig. S8 The band structures by using GGA+SOC with OOP magnetization at different strains.

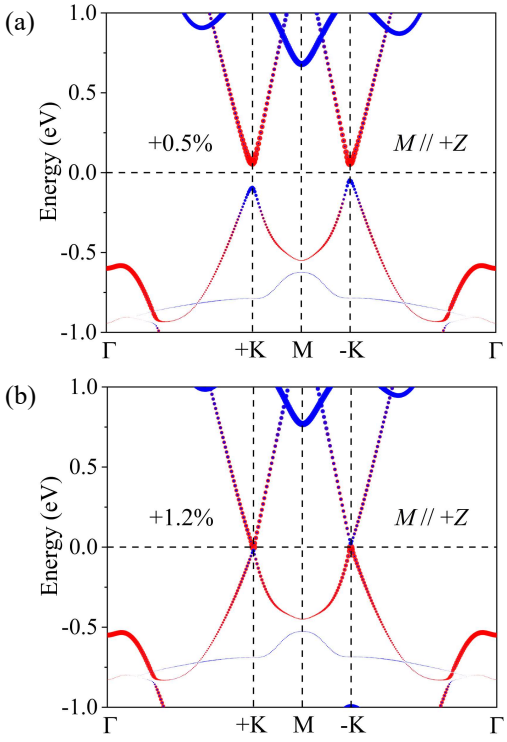

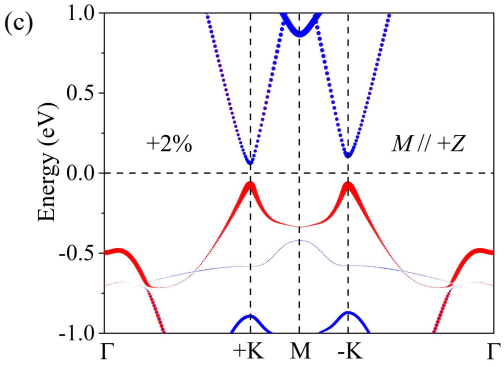

Fig. S9 For the $VCGeN_4$ with OOP magnetization, the V-d_{z^2} and $d_{x^2-y^2}/d_{xy}$ orbitals character band structures under (a) $\varepsilon = 0.5\%$, (b) $\varepsilon = 1.2\%$, and (c) $\varepsilon = 2\%$.

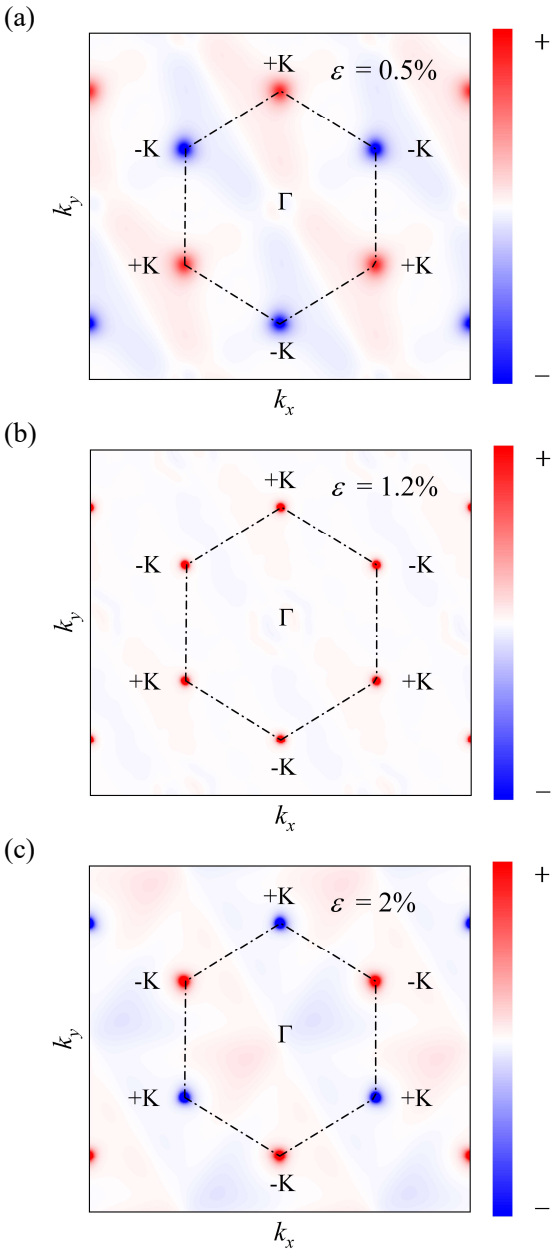

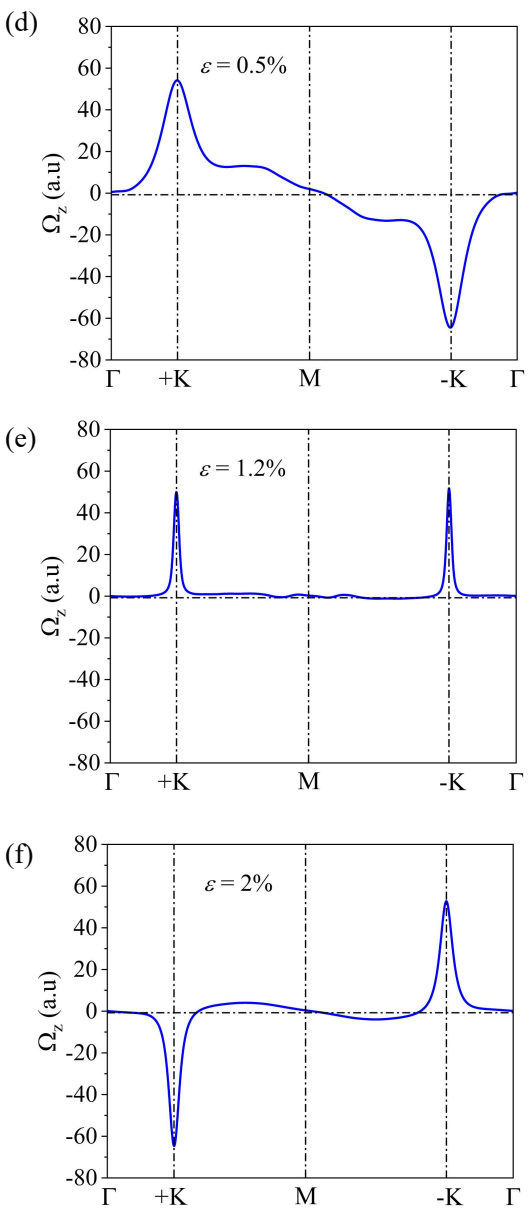

Fig. S10 The Berry curvature in the 2D BZ under (a) $\varepsilon = 0.5\%$, (b) $\varepsilon = 1.2\%$, and (c) $\varepsilon = 2\%$. The Berry curvature along the high symmetry points under (d) $\varepsilon = 0.5\%$, (e) $\varepsilon = 1.2\%$, and (f) $\varepsilon = 2\%$.

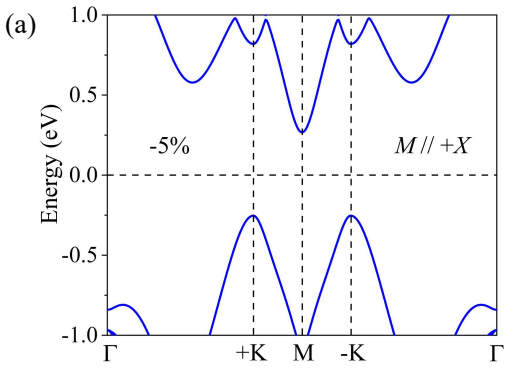

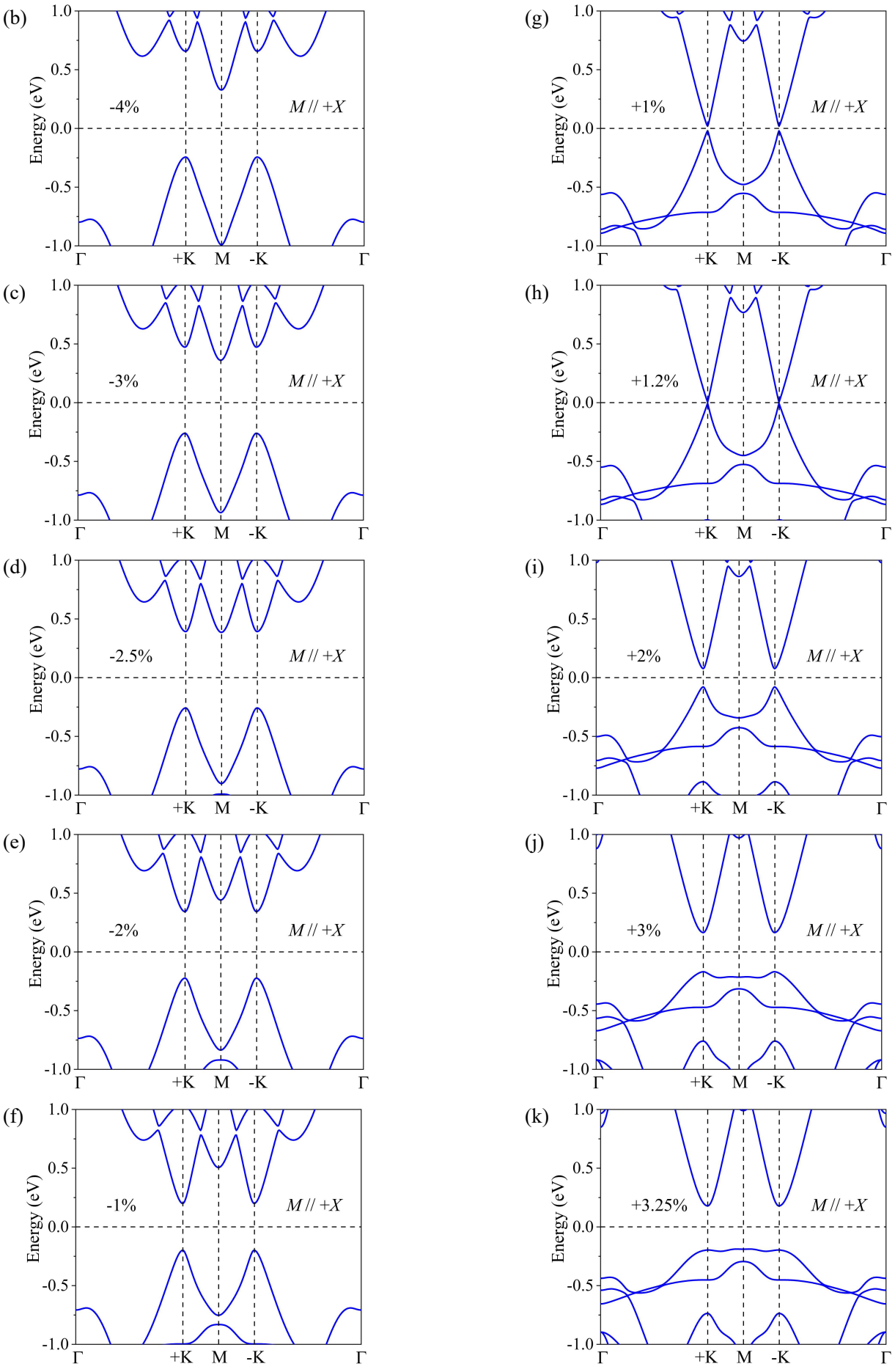
(b)
-4%
M // +X
(g)
+1%
M // +X
(c)
-3%
M // +X
(h)
+1.2%
M // +X
(d)
-2.5%
M // +X
(i)
+2%
M // +X
(e)
-2%
M // +X
(j)
+3%
M // +X
(f)
-1%
M // +X
(k)
+3.25%
M // +X
Energy (eV)
1.0
0.5
0.0
-0.5
-1.0
Γ
+K
M
-K
Γ

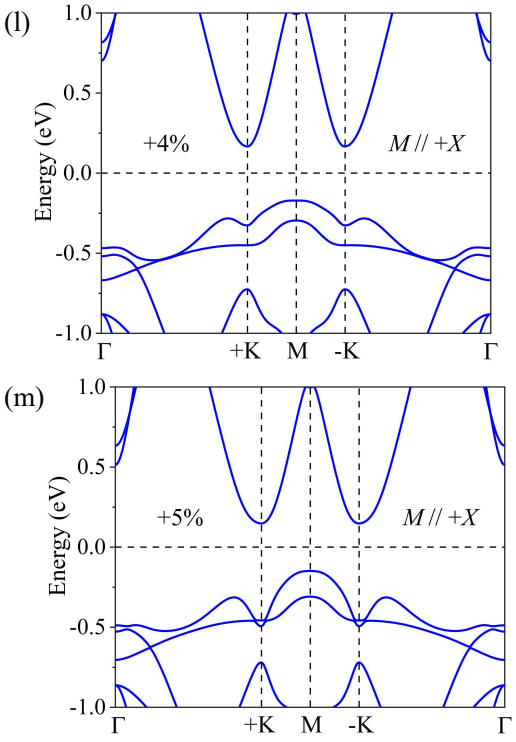

Fig. S11 The band structures by using GGA+SOC with IP magnetization at different strains.

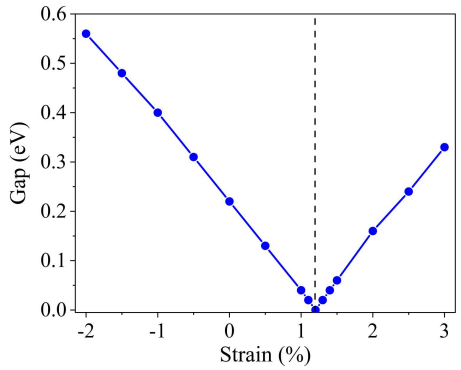

Fig. S12 The global band gaps with IP magnetization as a function of strain.

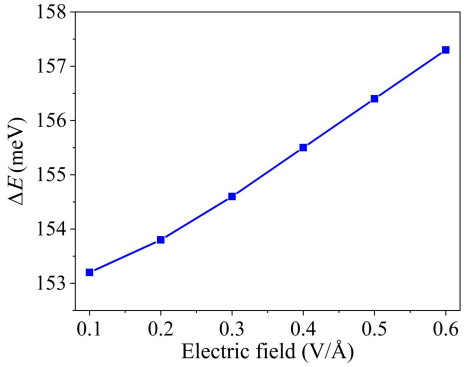

Fig. S13 The energy differences ($\Delta E = E_{AFM} - E_{FM}$) between FM and AFM configurations of $VCGeN_4$ as a function of electric field.

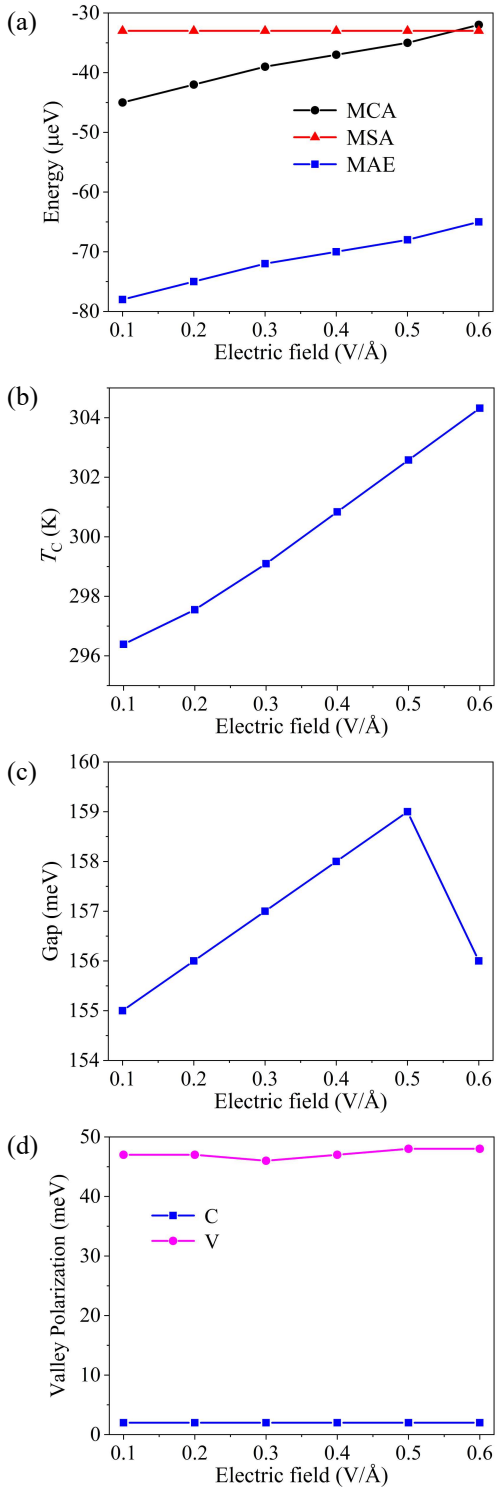

Fig. S14 For the $VCGeN_4$, (a) the MCA energy, MSA energy, and MAE as a function of electric field. (b) The T_C as a function of electric field. (c) The global band gap as a function of electric field. (d) The VP for the VB and CB as a function of electric field.

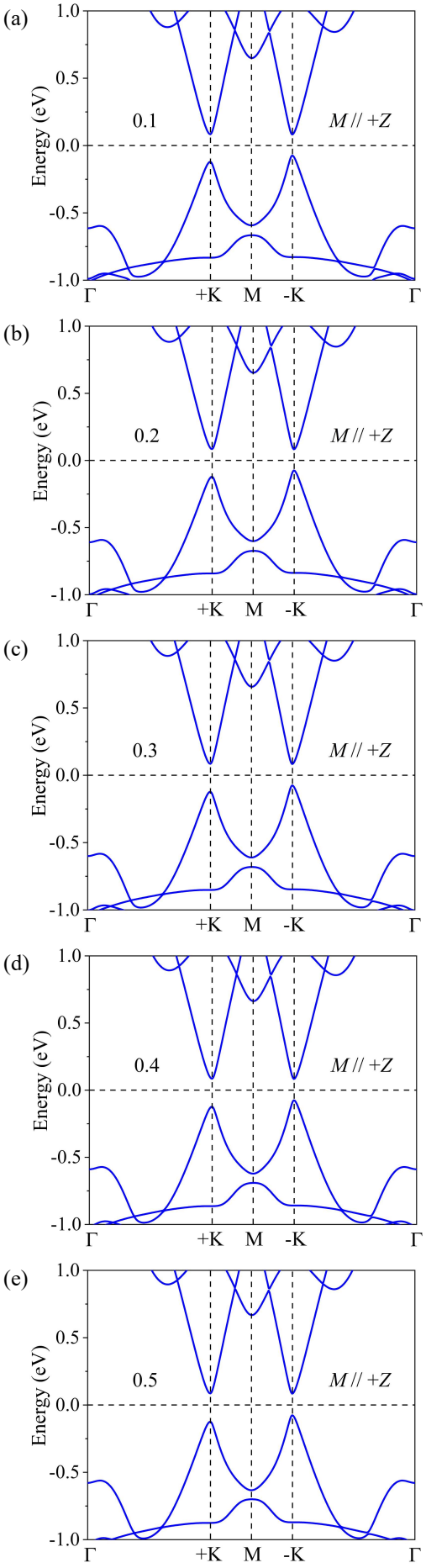

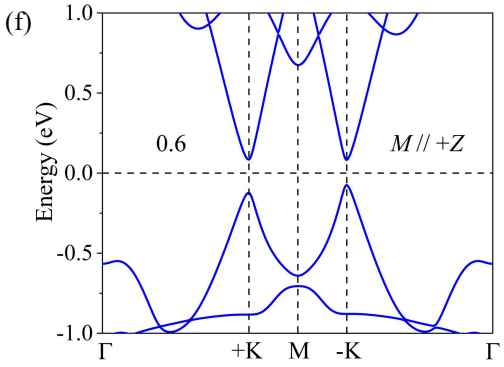

Fig. S15 For electric field E between 0.1 and 0.6 V/Å, the band structures by using GGA+SOC with OOP magnetization.

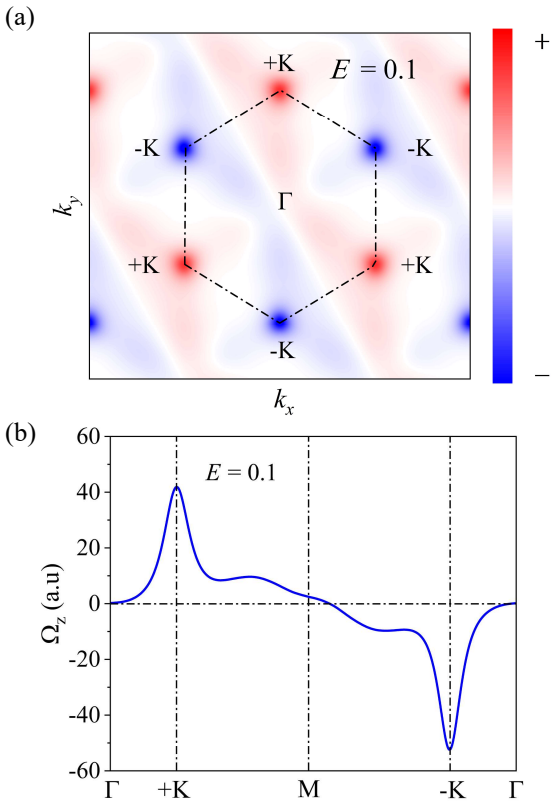

Fig. S16 For electric field $E = 0.1$ V/Å, the Berry curvature of $VCGeN_4$ (a) in the BZ and (b) along the high-symmetry points.